REPORT DOCUMENTATION PAGE

Form Approved OMB NO. 0704-0188

1. REPORT DATE (DD-MM-YYYY)	2. REPORT TYPE	3. DATES COVERED (From - To)
	New Reprint	-

4. TITLE AND SUBTITLE

Optimal battery charging, Part I: Minimizing time-to-charge, energy loss, and temperature rise for OCV-resistance battery model

5a. CONTRACT NUMBER
W911NF-10-1-0369

5b. GRANT NUMBER

5c. PROGRAM ELEMENT NUMBER
611102

6. AUTHORS

A. Abdollahi, X. Han, G.V. Avvari, N. Raghunathan, B. Balasingam, K. R. Pattipati, Y. Bar-Shalom

5d. PROJECT NUMBER

5e. TASK NUMBER

5f. WORK UNIT NUMBER

7. PERFORMING ORGANIZATION NAMES AND ADDRESSES

University of Connecticut - Storrs
438 Whitney Road Ext., Unit 1133

Storrs, CT 06269 -1133

8. PERFORMING ORGANIZATION REPORT NUMBER

9. SPONSORING/MONITORING AGENCY NAME(S) AND ADDRESS (ES)

U.S. Army Research Office
P.O. Box 12211
Research Triangle Park, NC 27709-2211

10. SPONSOR/MONITOR'S ACRONYM(S)
ARO

11. SPONSOR/MONITOR'S REPORT NUMBER(S)
57823-CS.120

12. DISTRIBUTION AVAILIBILITY STATEMENT

Approved for public release; distribution is unlimited.

13. SUPPLEMENTARY NOTES

The views, opinions and/or findings contained in this report are those of the author(s) and should not contrued as an official Department of the Army position, policy or decision, unless so designated by other documentation.

14. ABSTRACT

In this paper we present a closed-form solution to the problem of optimally charging a Li-ion battery. A combination of three cost functions is considered as the objective function: time-to-charge (TTC), energy losses (EL), and a temperature rise index (TRI). First, we consider the cost function of the optimization problem as a weighted sum of TTC and EL. We show that the optimal charging strategy in this case is the well-known Constant CurrenteConstant Voltage (CCeCV) policy with the value of the current in the CC stage being a function of the ratio of weighting on TTC and EL and of the resistance of the battery. Then,

15. SUBJECT TERMS

Battery charging,Optimal charging,Time to charge,Open circuit voltage,State of charge

16. SECURITY CLASSIFICATION OF:			17. LIMITATION OF ABSTRACT	15. NUMBER OF PAGES	19a. NAME OF RESPONSIBLE PERSON
a. REPORT	b. ABSTRACT	c. THIS PAGE			Yaakov Bar-Shalom
UU	UU	UU	UU		19b. TELEPHONE NUMBER 860-486-4823

Report Title

Optimal battery charging, Part I: Minimizing time-to-charge, energy loss, and temperature rise for OCV-resistance battery model

ABSTRACT

In this paper we present a closed-form solution to the problem of optimally charging a Li-ion battery. A combination of three cost functions is considered as the objective function: time-to-charge (TTC), energy losses (EL), and a temperature rise index (TRI). First, we consider the cost function of the optimization problem as a weighted sum of TTC and EL. We show that the optimal charging strategy in this case is the well-known Constant CurrenteConstant Voltage (CCeCV) policy with the value of the current in the CC stage being a function of the ratio of weighting on TTC and EL and of the resistance of the battery. Then, we extend the cost function to a weighted sum of TTC, EL and TRI and derive an analytical solution for the problem. It is shown that the analytical solution can be approximated by a CCeCV with the value of current in the CC stage being a function of ratio of weighting on TTC and EL, resistance of the battery and the effective thermal resistance.

REPORT DOCUMENTATION PAGE (SF298)
(Continuation Sheet)

Continuation for Block 13

ARO Report Number 57823.120-CS
Optimal battery charging, Part I: Minimizing time...

Block 13: Supplementary Note

Approved for public release; distribution is unlimited.

Journal of Power Sources xxx (2015) 1–11

Contents lists available at ScienceDirect

Journal of Power Sources

journal homepage: www.elsevier.com/locate/jpowsour

Optimal battery charging: Minimizing time-to-charge, energy loss, and temperature rise for OCV-resistance battery model

A. Abdollahi, X. Han, G.V. Avvari, N. Raghunathan, B. Balasingam*, K.R. Pattipati, Y. Bar-Shalom

Department of Electrical and Computer Engineering, University of Connecticut, 371 Fairfield Way, U-4157, Storrs, CT 06269, USA

HIGHLIGHTS

- Closed form solution for minimizing weighted sum of time-to-charge and energy loss.
- Semi-closed form solution by adding the temperature rise index to the cost function.
- Approximating temperature rise effect as a constant heating equivalent resistance.
- Analysis of efficiency performance of commercial batteries.

ARTICLE INFO

Article history:
Received 23 May 2014
Received in revised form
9 February 2015
Accepted 12 February 2015
Available online xxx

Keywords:
Battery charging
Optimal charging
Time to charge
Open circuit voltage
State of charge

ABSTRACT

In this paper we present a closed-form solution to the problem of optimally charging a Li-ion battery. A combination of three cost functions is considered as the objective function: time-to-charge (TTC), energy losses (EL), and a temperature rise index (TRI). First, we consider the cost function of the optimization problem as a weighted sum of TTC and EL. We show that the optimal charging strategy in this case is the well-known Constant Current–Constant Voltage (CC–CV) policy with the value of the current in the CC stage being a function of the ratio of weighting on TTC and EL and of the resistance of the battery. Then, we extend the cost function to a weighted sum of TTC, EL and TRI and derive an analytical solution for the problem. It is shown that the analytical solution can be approximated by a CC–CV with the value of current in the CC stage being a function of ratio of weighting on TTC and EL, resistance of the battery and the effective thermal resistance.

1. Introduction

Battery charging is a problem of significant interest, especially as the battery-dependent smart devices proliferate. The literature abounds with different strategies for charging batteries. Among the traditional methods of charging, the simplest is the constant trickle current charge strategy, which, due to its low charging current, requires a long charging time (around 10 h) [9]; constant current strategy with higher rates of current requires shorter charging time. The most widely-used traditional strategy is the constant-current constant-voltage (CC–CV) [9] strategy, in which a constant current is applied to the battery until the terminal voltage reaches a specified value, and afterward the charging current decreases by applying a constant voltage to the terminals of the battery. In Refs. [21,22], a multi-step constant-current charging is devised for shortening the charging time and prolonging the cycle life of the battery. Using orthogonal arrays, Taguchi-based methods for battery charging [12,23] present a systematic method to find the optimal solution with guidelines for choosing the design parameters. In Ref. [13], a boost charging strategy is proposed by applying very high currents to close-to-fully discharged batteries. In pulse-charging methods [6,7,17,20,27], the battery is exposed to very short rest or even deliberate discharging periods during the charging process. Soft-computing approaches are also used in the optimization of battery charging profile. In Ref. [24], the charging

* Corresponding author.
E-mail addresses: ali.abdollahi@uconn.edu (A. Abdollahi), xuh06002@engr.uconn.edu (X. Han), vinod@engr.uconn.edu (G.V. Avvari), niranjan.raghunathan@uconn.edu (N. Raghunathan), bala@engr.uconn.edu, bhalakumar@gmail.com (B. Balasingam), krishna@engr.uconn.edu (K.R. Pattipati), ybs@engr.uconn.edu (Y. Bar-Shalom).

http://dx.doi.org/10.1016/j.jpowsour.2015.02.075
0378-7753/

problem is viewed as an optimization problem with the objective function of maximizing the charge within 30 min using a multi-stage constant current charging algorithm whose optimal solution is obtained via an ant-colony approach. In Ref. [25], a universal voltage protocol is proposed to improve charging efficiency and cycle life by applying a charging profile depending on the state-of-health (SOH) of the battery, using SOH estimation approaches [26] in the optimization process. Recently, in Ref. [11], battery charging is considered as an optimization problem with cost function of time-to-charge and energy loss (as we do in this paper), but they have not solved the problem analytically; rather they have presented a numerical solution to the problem. Other approaches, such as genetic algorithm and neural network based strategies [16], data mining [2,10], and Grey-predicted charging system [8] have also been used for charging batteries.

In this paper we look at the charging problem from a fresh perspective using optimal control theory, and our goal is to find the optimal current profile that minimizes a specific cost function. In this sense, different objectives may be embedded in the cost function. One obvious cost function is the time-to-charge (TTC). We prefer to minimize the charging time as much as possible, as TTC reduction contributes to user satisfaction. Another important objective is the energy loss (EL) during charging. Reducing the energy loss increases the charging efficiency. In this paper, first we use an integrated cost function that includes both the TTC and EL. Then, we also include the effects of temperature into account, and the cost function is selected as a linear combination of three criteria: time-to-charge, energy loss, and temperature rise index (TRI). In both cases, analytical solutions of the optimal charging problem are derived.

The paper is organized as follows. In Section 2, we derive an analytical solution for the optimal charging current profile to minimize TTC and EL. In Section 3, we extend this approach to the case where temperature rise is considered as well. Section 4 is devoted to simulation results and finally we conclude the paper in Section 5.

2. Analytic solution for optimal charging current profile

We consider a simplified equivalent circuit model of the battery as shown in Fig. 1. The theory extends naturally to more complex models involving parallel RC elements (shown in Fig. 2), but analytical closed form solutions are not possible in the latter case. The model consists of a voltage source corresponding to the open-circuit voltage (OCV), which is dependent on the state of charge (SOC), and a resistance R_0. The SOC and OCV, are represented respectively by s and V_0. The OCV is a nonlinear function of SOC and is denoted by $V_0(s[k])$.

The state of charge is zero when the battery is totally discharged and it is one if it is completely charged. The sampling time is

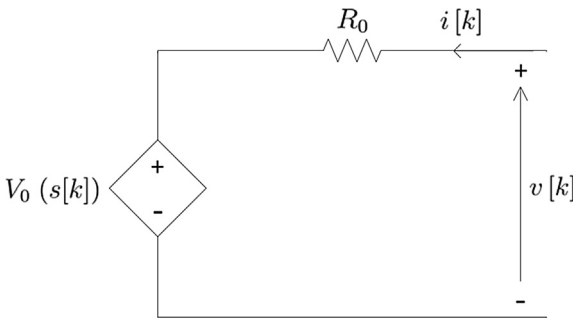

Fig. 1. Equivalent electrical circuit model I of battery.

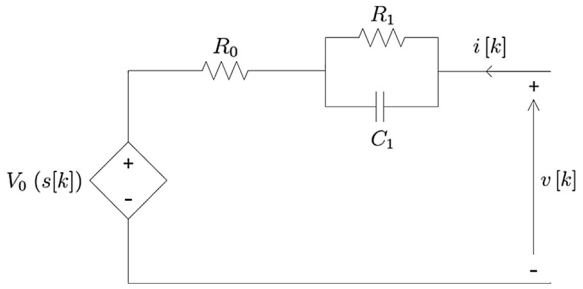

Fig. 2. Equivalent electrical circuit model III of battery.

denoted by Δ (in seconds). We assume that the initial and final SOC are known: $s[0] = s_0, s[k_f] = s_{k_f}$, where $k_f\Delta$ is the charging time. We also assume that the maximum allowed value of the terminal charging voltage is v_c, that is, $v[k] \le v_c$ for all k.

The SOC dynamics for the battery considering the foregoing model are as follows:

$$s[k+1] = s[k] + c_h i[k] \tag{1}$$

where c_h (in 1/Amperes) is the parameter in Coulomb counting, given by

$$c_h = \frac{\Delta}{3600 C_{\text{batt}}} \tag{2}$$

where C_{batt} (in Ah) is the battery capacity, assumed to be known.

Let the objective function be a combination of TTC and EL. In other words,

$$\tilde{J}_{\text{tE}} = w_{\text{t}} J_{\text{t}} + w_{\text{E}} J_{\text{E}} = w_{\text{t}} k_f \Delta + w_{\text{E}} \sum_{k=0}^{k_f-1} R_0 i^2[k]\Delta \tag{3}$$

where J_{t} is the TTC cost function, J_{E} is the EL cost function; w_{t} and w_{E} are weights on the TTC and EL cost functions, respectively. The resistance of the battery, i.e., R_0, is assumed to be known.

The charging problem then could be formulated as follows:

Minimize $\tilde{J}_{\text{tE}}$ subject to:

$$s[k+1] = s[k] + c_h i[k] \quad s[0] = s_0 \quad s\left[k_f\right] = s_{k_f} \tag{4}$$

$$V_0\ (s[k]) + R_0 i[k] \le v_{\max} \tag{5}$$

$$i[k] \le i_{\max} \tag{6}$$

It is important to note that only the ratio of weights affects the optimal current profile of $i[k]$. Therefore, by dividing (3) by w_{E}, we redefine the cost function as follows:

$$J_{tE} = \tilde{J}_{tE} \big/ w_E = \rho_t J_t + J_E = \rho_t k_f \Delta + \sum_{k=0}^{k_f-1} R_0 i^2[k]\Delta \tag{7}$$

where $\rho_{\text{t}} = w_{\text{t}}/w_{\text{E}}$. Also note that when the current is injected into the battery, the V_0 starts to increase and this, in turn, causes the terminal voltage to rise, until it reaches $v_{\max}$, which is the maximum allowed terminal voltage. During the whole charging process the current should not exceed $i_{\max}$, which is the maximum allowed charging current. In this paper, we use v_c for $v_{\max}$, where v_c is the voltage corresponding to SOC of 1; that is

$$v_c = V_0(1) \tag{8}$$

Assume that at time k_1, the terminal voltage $v[k_1]$ reaches v_c and let us denote the state of charge at time k_1 as s_1. After time k_1, the terminal voltage should be fixed at the constant voltage (CV) v_c; hence, for $k = k_1, k_1+1, \ldots, k_f - 1$, the dynamics of the system are as follows:

$$i[k] = \frac{1}{R_0}(v_c - V_0(s[k])) \tag{9}$$

$$s[k+1] = s[k] + c_h i[k] \tag{10}$$

$$s[k_1] = s_1 \quad s\left[k_f\right] = s_{k_f} \tag{11}$$

Before going further, let us define a new equivalent problem as follows:

Minimize

$$J_{tE} = \rho_t J_t + J_E = \rho_t k_1 \Delta + \sum_{k=0}^{k_1-1} R_0 i^2[k]\Delta \tag{12}$$

subject to:

$$s[k+1] = s[k] + c_h i[k] \quad s[0] = s_0 \quad s[k_1] = s_1 \tag{13}$$

This problem is in fact the minimization in the stage where the terminal voltage is below v_c and therefore here the condition $V_0\,(s[k]) + R_0 i[k] \le v_c$ is not shown as we know that it holds.

Inspired by Refs. [18] and [1], we solve the problem in three steps as described below:

❶ Given k_1 (when the terminal voltage constraint becomes active), find the optimal current profile that minimizes the energy losses, and calculate the corresponding energy losses as a function of k_1.
❷ Generate a new equivalent cost function J_{tE^*} consisting of the weighted TTC plus the k_1-dependent minimum energy loss obtained in step 1, and find the optimal k_1 based on this cost function.
❸ Given the optimal k_1 from step 2, evaluate the optimal current obtained in step 1.

In the first step, assuming k_1 is known, we find the optimal current $i^*[k|k_1]$ that minimizes the energy loss. Having this optimal current profile, we can calculate the minimum EL cost function $J_E^*(k_1)$, which is a function of k_1. In the second step, we use the partially optimized cost function $J_{tE^*} = \rho_t k_1 \Delta + J_E^*(k_1)$ and we find the optimum value for k_1, say k_1^*. In the third step, we insert the optimal final time k_1^* into the current $i^*[k|k_1]$ (obtained in step 1) to find the optimal current $i^*[k]$. The final result will be $J_{tE}^*(k_1^*)$.

The first stage is formulated as follows:

Minimize

$$J_E(k_1) = \sum_{k=0}^{k_1-1} R_0 i^2[k]\Delta \tag{14}$$

subject to

$$s[k+1] = s[k] + c_h i[k] \quad s[0] = s_0 \quad s[k_1] = s_1 \tag{15}$$

The Hamiltonian function for this problem is

$$H[k] = R_0 i^2[k]\Delta + \lambda[k+1](s[k] + c_h i[k]) \tag{16}$$

The following equations must hold for the optimal solution [5]:

$$\frac{\partial H[k]}{\partial i[k]} = 0 \tag{17}$$

$$\lambda[k] = \frac{\partial H[k]}{\partial s[k]} \tag{18}$$

$$s[k+1] = \frac{\partial H[k]}{\partial \lambda[k+1]} \tag{19}$$

From (17) we have

$$i^*[k] = -\frac{c_h \lambda[k+1]}{2R_0\Delta} \quad k = 0, 1, \ldots k_1 - 1 \tag{20}$$

From (18), we can write

$$\lambda[k] = \lambda[k+1] \quad k = k_1 - 1, \ldots, 0 \quad \lambda[k_1] = \nu \tag{21}$$

where ν is the Lagrange multiplier associated with the constraint $s[k_1] = s_1$. Equation (21) implies that all co-states are equal; therefore, we can write

$$\lambda[k] = \nu \quad k = 0, 1, \ldots k_1 \tag{22}$$

Based on (22), equation (20) can be written as

$$i^*[k] = -\frac{c_h \nu}{2R_0\Delta} \quad k = 0, 1, \ldots, k_1 - 1 \tag{23}$$

Note that equation (23) states that the optimal current is constant. From (19), we can write

$$s[k+1] = s[k] + c_h i[k] \tag{24}$$

which is actually the dynamics of the system. Knowing the initial state of charge (s_0), and noting the optimal current in (23) is constant, we have

$$s[k] = s_0 + c_h \sum_{l=0}^{k-1} i[l] = s_0 - \frac{k c_h^2 \nu}{2R_0\Delta} \tag{25}$$

Since for $k = k_1$ we have $s[k_1] = s_1$, therefore

$$s_1 = s_0 - \frac{k_1 c_h^2 \nu}{2R_0\Delta} \tag{26}$$

Solving for ν, we have

$$\nu = -\frac{2R_0\Delta(s_1 - s_0)}{k_1 c_h^2} \tag{27}$$

Inserting (27) into (23), we have

$$i^*[k] = \frac{s_1 - s_0}{k_1 c_h} \quad k = 0, 1, \ldots, k_1 - 1 \tag{28}$$

Inserting (28) into the cost function, the optimal cost function, given k_1 is:

$$J_E^*(k_1) = \sum_{k=0}^{k_1-1} R_0 \left(\frac{s_1 - s_0}{k_1 c_h}\right)^2 \Delta = \frac{R_0\Delta(s_1 - s_0)^2}{k_1 c_h^2} \tag{29}$$

Now, consider step 2 and define the cost function as

$$J_{tE^*} = \rho_t k_1 \Delta + J_E^*(k_1) = \rho_t k_1 \Delta + \frac{R_0\Delta(s_1 - s_0)^2}{k_1 c_h^2} \tag{30}$$

To find the optimum k_1, the following relations should hold:

Please cite this article in press as: A. Abdollahi, et al., Journal of Power Sources (2015), http://dx.doi.org/10.1016/j.jpowsour.2015.02.075

$$J_{tE^*}(k_1-1) \geq J_{tE^*}(k_1) \tag{31}$$

$$J_{tE^*}(k_1+1) \geq J_{tE^*}(k_1) \tag{32}$$

Inserting (30) into (31) and (32) we obtain two second-order equations in term of k_1. Solving these equations, we get k_1^- and k_1^+, respectively, for relations (31) and (32).

$$k_1^{\mp} = \frac{\pm 1 + \sqrt{1 + \frac{4R_0(s_1-s_0)^2}{\rho_t c_h^2}}}{2} \tag{33}$$

The optimum k_1 is ceil(k_1^-) or floor(k_1^+). Since $k_1^- - k_1^+ = 1$, we have ceil(k_1^-) = floor(k_1^+) = round($(k_1^- + k_1^+)/2$). Thus,

$$k_1^* = \text{round}\left(\sqrt{\frac{1}{4} + \frac{R_0(s_1-s_0)^2}{\rho_t c_h^2}}\right) \tag{34}$$

A more convenient way is to treat k_1 in (30) as a continuous variable and take derivative of (30) with respect to k_1 as follows:

$$\frac{\partial J_{tE^*}(k_1)}{\partial k_1} = \rho_t \Delta - \frac{R_0 \Delta (s_1-s_0)^2}{k_1^2 c_h^2} = 0 \tag{35}$$

$$k_1^* = \frac{s_1-s_0}{c_h}\sqrt{\frac{R_0}{\rho_t}} \tag{36}$$

Note that if we neglect 1/4 in (34), the argument of the rounded function in (34) is exactly the same as the one in (36).

Step 3 involves inserting (36) into (28) to find the optimum current

$$i^*[k] = \frac{s_1-s_0}{k_1^* c_h} = \sqrt{\frac{\rho_t}{R_0}} \quad k = 0, 1, \ldots, k_1 - 1 \tag{37}$$

It is seen that the optimal current is constant and is a function of the weight on TTC and the series resistance. Therefore, the solution of optimal time-to-charge and energy loss (OtE) problem is a CC–CV profile with the current of the CC stage given by (37). Following the CC stage, from k_1 to k_f, one has the CV stage where

$$v[k] = v_c \quad k = k_1, \ldots, k_f \tag{38}$$

To the best of our knowledge, this is the first time that it is proved that the well-known CC–CV charging profile is the optimal solution of a particular optimization problem, namely, the problem of minimizing the weighted sum of time-to-charge and energy loss.

In the sequel, this profile is referred to as OtE profile or OtE policy.

Before we close this section, we point out another way of solving the OtE problem of (12) and (13) by condensing (13) for all values of k into a single condition. From (13) we can write

$$i[k] = (s[k+1] - s[k])/c_h \tag{39}$$

Since (39) holds for $k = 0, 1, \ldots, k_1 - 1$, and using the initial and end values of SOC from (13) we can write:

$$\sum_{l=0}^{k_1-1} i[l] = (s_1 - s_0)/c_h \tag{40}$$

Therefore, the problem of (12) and (13) is equivalent to a quadratic programming problem with the constraint in (40). In this way, we are dealing with currents $i[l]$ as our unknowns. It is easy to show that this results in the same solution as (37). This simplification of the dynamics of the system into the condensed condition of (40) will be useful in the next section where we derive an analytical solution when the cost function includes the summation of temperature rises as well.

It should be noted that the practical meaning of the parameters of optimization problem (e.g., w_t and w_E in (3) and ρ_t in (12)) is to use them in an iterative design procedure to reach the desired performance. For example, if the maximum allowed energy loss is E_{max} and the maximum acceptable time-to-charge is TTC_{max}, then in the design procedure, w_t and w_E should be selected inversely proportional to TTC_{max} and E_{max}, respectively; that is $w_t \propto 1/TTC_{max}$, $w_E \propto 1/E_{max}$ and then iterate. Or equivalently, ρ_t should be selected proportional to E_{max}/TTC_{max}; that is $\rho_t \propto E_{max}/TTC_{max}$ and then iterate on the proportionality factor. As E_{max}/TTC_{max} is approximately, the allowable average power loss, ρ_t should be selected proportional to allowable average power loss.

3. Optimal charging problem considering temperature

In this section, we will extend the cost function to include the battery temperature via temperature rise index (TRI, to be defined) as well as TTC and EL. To this end, we need a temperature model for the battery. Refs [15] and [19] describe the temperature model of the battery as a linear system with two states, namely, T_{core} and T_{air}, and reference [14] uses the nonlinear heat transfer equation with a single state. Simulations show that the dynamics of T_{air} have negligible fluctuations around the ambient temperature. Therefore, the temperature model, considered below, can be simplified to the linear part of the heat transfer equation

$$T[k+1] = T[k] - a(T[k] - T_{amb}) + bi^2[k] \tag{41}$$

where

$$a = \frac{\Delta}{m_{batt} C_{h,batt} R_{Eff}} \tag{42}$$

is the cooling coefficient and

$$b = \frac{R_0 \Delta}{m_{batt} C_{h,batt}} \tag{43}$$

Here T is the battery core temperature in kelvin (K), T_{amb} is the ambient temperature in K, m_{batt} is the battery mass in kg, $C_{h,batt}$ is the heat capacity of the battery in J/(kg·K), and R_{Eff} is the effective thermal resistance in K/W (kelvin/watt).

Defining temperature rise (TR) as $\tilde{T}[k] = T[k] - T_{amb}$ and assuming $T[0] = T_{amb}$, we can write

$$\tilde{T}[k+1] = (1-a)\tilde{T}[k] + bi^2[k], \quad \tilde{T}[0] = 0 \tag{44}$$

The solution of (44) is

$$\tilde{T}[k] = b\sum_{l=0}^{k-1} (1-a)^{k-1-l} i^2[l] \tag{45}$$

Equation (45) states that the temperature rise at any time is the integral of the square of current, from time zero up to that time with a "forgetting factor" of $(1-a)$ and the scaling factor b.

Since $\tilde{T}[k]$ is positive for any k, the cost function including TTC, EL and TR can be written as

$$J_{tET} = \rho_t J_t + J_E + \rho_T J_T \tag{46}$$

where J_t and J_E are TTC and EL as before and J_T is the temperature rise index (TRI) defined as follows:

$$J_T = \Delta \sum_{k=0}^{k_f} \tilde{T}[k] \tag{47}$$

Since $\tilde{T}[0] = 0$, the TRI can be written as

$$J_T = \Delta \sum_{k=0}^{k_f-1} \tilde{T}[k+1] \tag{48}$$

Using (45) and (48), we can write (46) as follows

$$\begin{aligned} J_{tET} &= \rho_t k_f \Delta + \sum_{k=0}^{k_f-1} R_0 i^2[k]\Delta \\ &+\rho_T b \Delta \sum_{k=0}^{k_f-1} \sum_{l=0}^{k} (1-a)^{k-l} i^2[l]\Delta \end{aligned} \tag{49}$$

which can be simplified as follows

$$J_{tET} = \rho_t k_f \Delta + \Delta \sum_{k=0}^{k_f-1} \left(R_0 + \rho_T b \sum_{l=0}^{k_f-k-1} (1-a)^l \right) i^2[k] \tag{50}$$

Simplifying the inner summation and noting that $b/a = R_0 R_{Eff}$, we can write

$$J_{tET} = \rho_t k_f \Delta + \Delta \sum_{k=0}^{k_f-1} R_{eq}[k] i^2[k] \tag{51}$$

$$R_{eq}[k] = R_0 + R_T[k] \tag{52}$$

$$R_T[k] = \rho_T R_0 R_{Eff} \left(1 - (1-a)^{k_f-k}\right) \tag{53}$$

where $R_T[k]$ is the heating equivalent resistance. Assume, as before, that at time k_1, the terminal voltage v reaches its maximum allowable value of v_c, and SOC reaches s_1. Given s_1 and k_1, we can write the cost function as

$$J(s_1, k_1) = \Delta \sum_{k=0}^{k_1-1} R_{eq}[k] i^2[k] \tag{54}$$

Note that we discarded the contributions of $i[k_1], \ldots, i[k_f - 1]$, because when the terminal voltage reaches v_c the current is already determined by the constrained dynamics of the system in (9); we also discarded the contribution of k_f, i.e. $\rho_t k_f \Delta$, because: firstly, k_1 is given; secondly, given s_1, $k_f - k_1$ is also known, which means k_f is known. An important point to note is that, while the upper bound of the summation in (54) is $k_1 - 1$, the formulation for R_{eq}, i.e., (52), considers the effect of the whole charging time and it contains k_f rather than k_1.

Now, given s_1 and k_1, we can state the optimal charging problem as follows: Minimize (54) subject to (40), or equivalently

$$\text{Minimize}: \quad L = J(s_1, k_1) + \lambda \left(\sum_{l=0}^{k_1-1} i[l] - \frac{s_1 - s_0}{c_h} \right) \tag{55}$$

Taking the derivative of Lagrangian L with respect to $i[k]$ for $k = 0, 1, \ldots, k_1 - 1$ and equating it to zero, we have:

$$i[k] = -\frac{\lambda}{2R_{eq}[k]\Delta} = -\frac{\lambda G_{eq}[k]}{2\Delta} \tag{56}$$

where $G_{eq}[k] = 1/R_{eq}[k]$ is the conductance. Taking the derivative of L with respect to λ, and using (56) we find the optimal current profile in the first stage as follows:

$$i^*[k] = -\frac{G_{eq}[k](s_1 - s_0)}{c_h \sum_{k=0}^{k_1-1} G_{eq}[k]} \quad k = 0, 1, \ldots, k_1 - 1 \tag{57}$$

We refer to the current profile in (57) as the optimal time-to-charge, energy losses and temperature rise (OtET) policy. Note that (57) is similar to what we obtained for the OtE case. In particular, if $\rho_T = 0$, then (57) will be the same as (28). Also, comparing (56) with the OtE case and noting that for $k = 0, 1, \ldots, k_1 - 1$ we can use the approximation of $R_{eq}[k] \approx R_0(1 + \rho_T R_{Eff})$, analogous to the optimal current profile of (37), we can write

$$i^*[k] \approx \sqrt{\frac{\rho_t}{R_0\left(1 + \rho_T R_{Eff}\right)}} \quad k = 0, 1, \ldots, k_1 - 1 \tag{58}$$

We refer to the current profile of (58) as the near-optimal time-to-charge, energy loss and temperature rise (NOtET) policy.

4. Simulations

In this section, we present simulations based on the theoretical foundations of the previous section.

4.1. Verification of the optimal solution

Here, we apply different levels of current and the simulation is run until the terminal voltage reaches v_c and after that a constant voltage of v_c is applied until the battery is charged to s_{k_f}. Five different current profiles are chosen including the optimal current profile (Fig. 3). The optimal current profile as mentioned before has the value of $\sqrt{\rho_t/R_0}$ in the CC stage. The battery parameters of Nokia BP-4L (Cell#3), given in the appendix, are used. The following simulation parameters are used: $\rho = 1$, $\Delta = 1$(s), $s_0 = 0$, $s_{k_f} = 1$.

The appendix also shows the parameters of the OCV curve (calculated based on [3]). The OCV is a function of SOC s as in Ref. [3].

$$z(s) \triangleq E + s(1 - 2E) \tag{59}$$

$$\begin{aligned} OCV(z) = K_0 + K_1 z^{-1} + K_2 z^{-2} + K_3 z^{-3} + K_4 z^{-4} + K_5 z + K_6 \ln(z) \\ + K_7 \ln(1 - z) \end{aligned} \tag{60}$$

and $E = 0.15$. Fig. 3 shows the current profiles with different levels of current in the CC stage. As seen from Fig. 3, at lower levels of current, the CC stage will take a longer time and the terminal voltage reaches the threshold voltage of v_c at a later time. At higher levels of current, however, the OCV grows more rapidly. As the terminal voltage is $v[k] = V_0\,(s[k]) + R_0 i[k]$, at higher levels of current the threshold voltage of v_c is reached in a shorter time.

Fig. 4(a) shows the cost function J_{tE} for the five current profiles of Fig. 3 and Fig. 4(b) shows the corresponding current levels in the CC stage. It is seen that the optimal current profile (i.e., profile 3) has the lowest cost function. Deviating from this profile, either by increasing or decreasing the current in the CC stage, results in an increase in the cost function. For the lower current levels (profiles 1–2), the rise in the cost function is due to a rise in TTC and for higher current levels (profiles 4–5) the rise in cost function is due to rise in EL.

Please cite this article in press as: A. Abdollahi, et al., Journal of Power Sources (2015), http://dx.doi.org/10.1016/j.jpowsour.2015.02.075

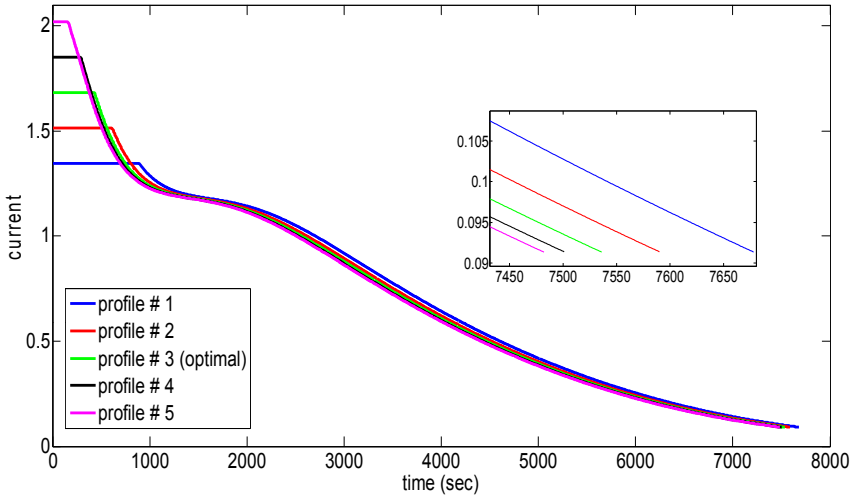

Fig. 3. Five different current profiles (including the optimal profile).

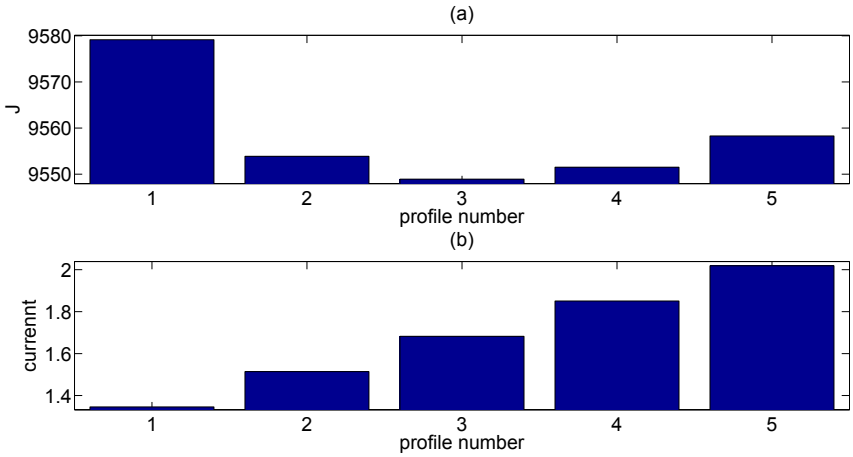

Fig. 4. Five different current profiles: a) cost functions b) current levels in CC stage.

4.2. Effect of weights

In this subsection, we use different cost functions and find the corresponding optimal profiles. Different values of ρ_t from 0.1 to 0.5 are chosen. Figs. 5–7, respectively, show the profiles of current, state of charge and terminal voltage. Fig. 5 shows that low values of ρ_t result in low values of current in the CC stage. In other words, a low ρ_t puts less emphasis on charging time and more emphasis on the energy losses; hence, it results in low level of current which provides low energy losses. On the other hand, by increasing ρ_t, more emphasis is placed on the charging time. Consequently, the level of current is increased proportionally to $\sqrt{\rho_t}$ to reduce the TTC.

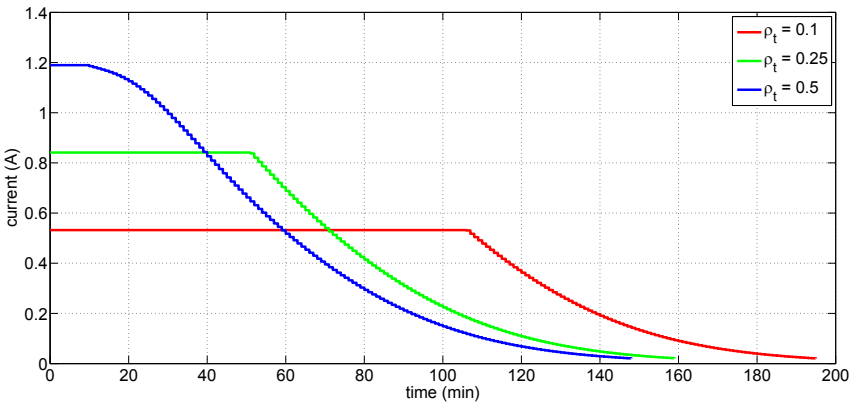

Fig. 5. Current profiles for different values of ρ_t.

Please cite this article in press as: A. Abdollahi, et al., Journal of Power Sources (2015), http://dx.doi.org/10.1016/j.jpowsour.2015.02.075

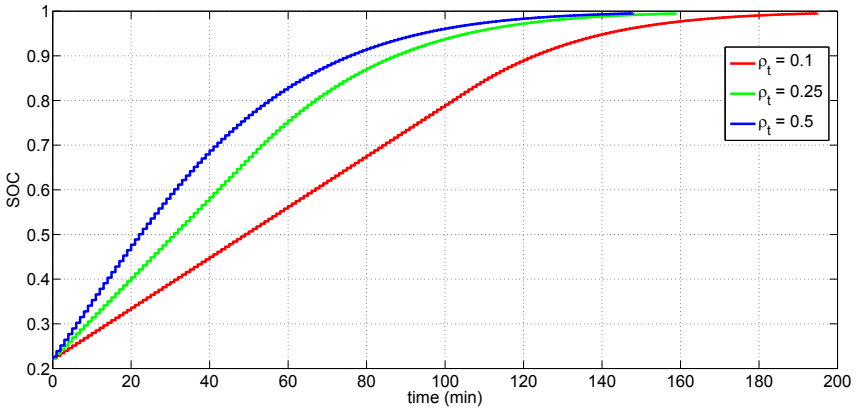

Fig. 6. SOC profiles for different values of ρ_t.

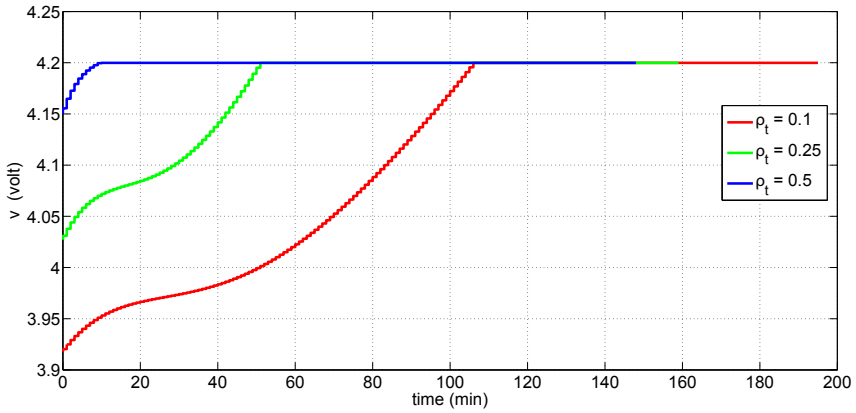

Fig. 7. Voltage profiles for different values of ρ_t.

Fig. 6 shows the state-of-charge profiles for different values of ρ_t. It is seen that by increasing ρ_t, more emphasis is placed on charging time and the SOC reaches the final value in a shorter time. Fig. 7 shows the terminal voltage profiles for different values of ρ_t. Note that for low values of ρ_t, as the emphasis on energy loss is high, the corresponding current level in the CC stage is low, and consequently, the terminal voltage reaches the threshold value of v_c at a later time. Hence, the duration of the CC stage is high and the charging time is high as well.

Fig. 8 shows the time-to-charge, energy losses and efficiency as functions of ρ_t. As expected, high values of ρ_t result in lower TTC. The low TTC, however, is obtained by increasing the current level; as EL is proportional to the square of current, thus the high values of ρ_t result in high values of EL. The high values of EL mean that a higher fraction of input power is wasted; hence it is equivalent to a decline in efficiency.

Fig. 9 shows the time-to-charge versus efficiency (ratio of effective to total energy) curve. TTC and efficiency are two counteracting objectives. For low values of ρ_t, as less emphasis is put on TTC, the TTC is high; however, high TTC is the result of low current

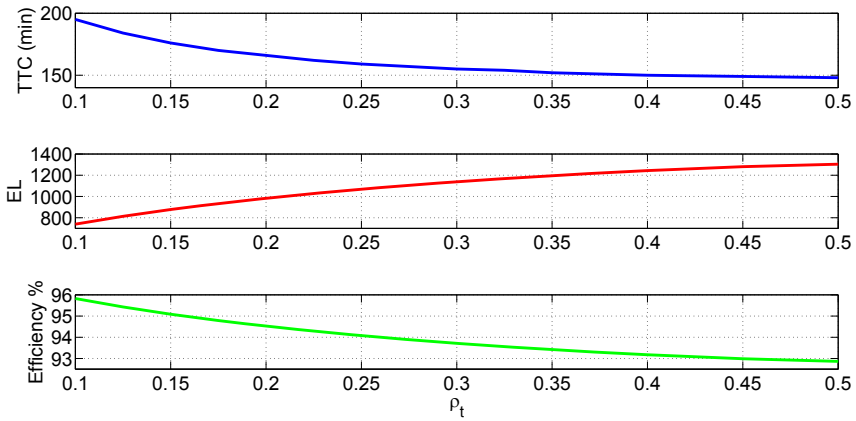

Fig. 8. TTC, EL and efficiency curves for different values of ρ_t.

Please cite this article in press as: A. Abdollahi, et al., Journal of Power Sources (2015), http://dx.doi.org/10.1016/j.jpowsour.2015.02.075

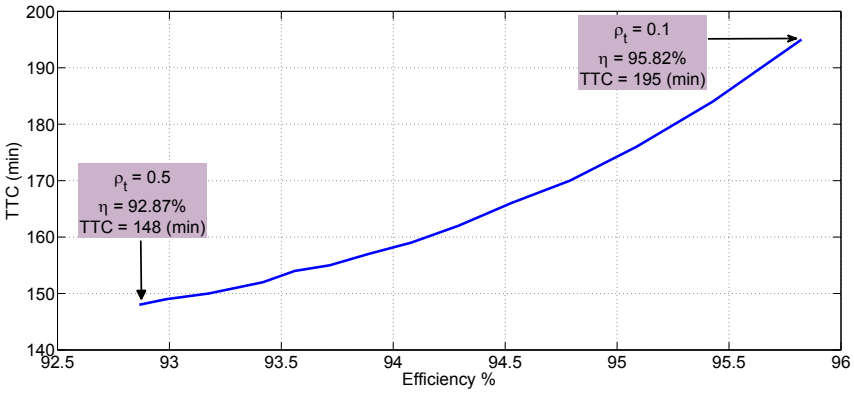

Fig. 9. TTC versus efficiency.

Table 1
Battery thermal parameters.

Paramter set	m_{batt} (kg)	R_{Eff} (K/W)	$C_{h,batt}$ (J/(kg·K))
A	0.37824	7.8146	795
B	0.080	1.6528	168.15

Table 2
Cost function for different schemes.

ρ_t	ρ_T	Thermal parameters	J_{tET}		
			OtE	NOtET	OtET
1	1	A	26,734	22,206	22,198
1	4	A	72,023	38,996	38,960
1	1	B	14,970	14,696	14,696
1	4	B	24,966	21,272	21,271

values, which incur low energy losses and hence higher efficiency. For example at $\rho_t = 0.1$, the TTC is 195 min, but the efficiency is as high as 95.82%. On the other hand, for high values of ρ_t which place more emphasis on TTC, the TTC is reduced dramatically; however, low TTC is achieved by increasing the current values, which results in high energy losses and hence lower efficiency. For example, at $\rho_t = 0.5$, the TTC is as low as 148 min, but the efficiency decreases to 92.87%.

4.3. Temperature effect

In this section, we consider the effect of temperature rise index (TRI) on optimal charging. The cost function is a weighted sum of TTC (seconds), EL (Joules) and TRI (Kelvin seconds), given by

$$J_{tET} = \rho_t \times TTC + EL + \rho_T \times TRI \tag{61}$$

We used two sets of thermal parameters, shown in Table 1. Parameter set "A" is adopted from Ref. [19]. Parameter set "B" is a scaled version of parameter set "A" with m_{batt} set as the weight of Nokia BP-4L. For each set of thermal parameters ("A" or "B"), the weights of the cost function are chosen as $\rho_t = 1$, $\rho_T = 1$ and $\rho_t = 1$, $\rho_T = 4$. Three schemes are used: OtE (equations (37) and (38)), OtET (equations (38) and (57)), and NOtET (equations (38) and (58)). The cost function in (61) or (46) is calculated for the three schemes. Table 2 shows the cost functions of the three schemes for different weightings. As seen from this table, the cost function for the OtE has the highest value. Also the difference between the cost function of OtET and NOtET is negligible with the OtET being slightly smaller when thermal parameter set "A" is used. For thermal parameter set of "B", there is visually no difference between NOtET and OtET. Due to this negligible difference in the cost function and also since the calculation of NOtET profile is much easier than that of the OtET, it is reasonable to use NOtET rather than the OtET scheme. Also note that the weight on TRI results in a reduction of current, as can be seen from Fig. 10. This reduction in current level results in a lower temperature rise (see Fig. 11). In other words, energy losses with R_{eq} instead of R_0 can be used as a surrogate cost function for the TRI.

4.4. Analysis of different commercial batteries

In this section, we discuss the behavior of different commercial batteries. The parameters of the investigated batteries are given in

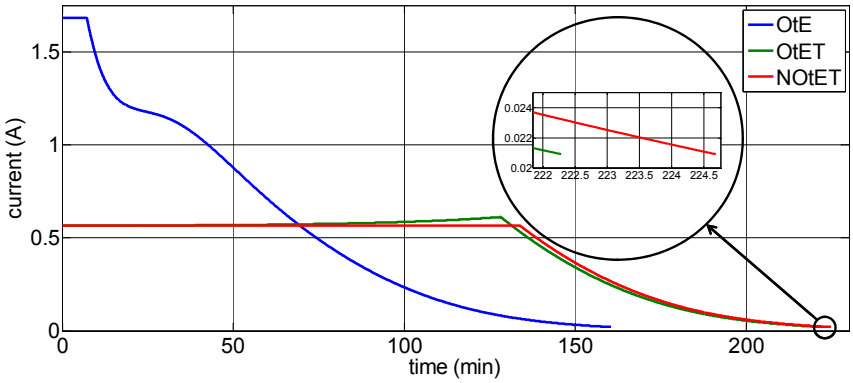

Fig. 10. Current profiles for $\rho_t = 1, \rho_T = 1$ and temperature parameter set "A".

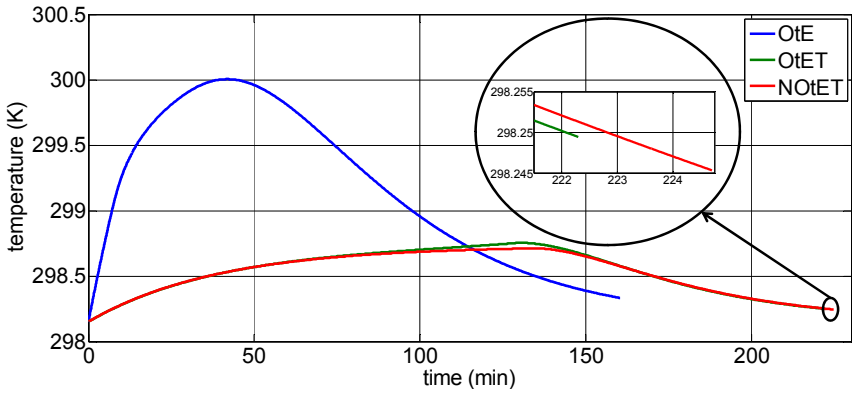

Fig. 11. Temperature profiles for $\rho_t = 1, \rho_T = 1$ and temperature parameter set "A".

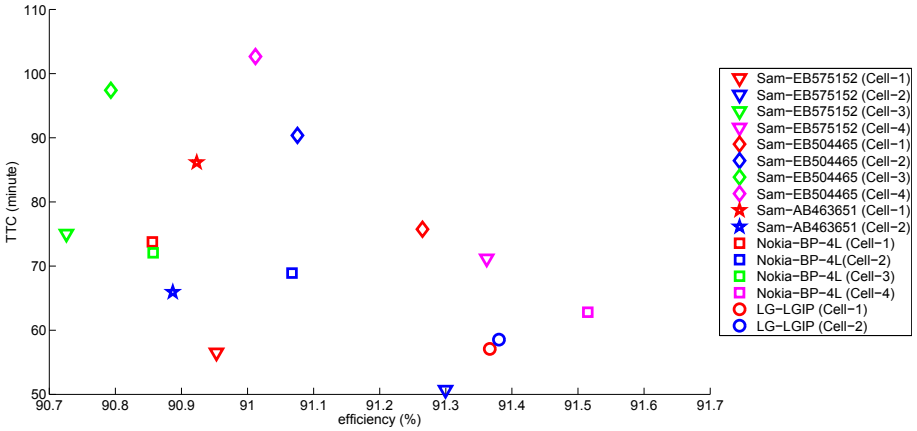

Fig. 12. Time to charge versus efficiency of different battery types at 25 °C.

the appendix. Note that the equivalent electrical circuit parameters given in Table 3 are for model III (see Fig. 2). In simulations, we use the summation of "$R_0 + R_1$" of model III as an estimate of resistance R_0 in model I. The batteries are Samsung EB575152 (four cells), Samsung EB504465 (four cells), Samsung AB463651 (two cells), Nokia BP-4L (four cells), LG LGIP (two cells).

Next, we apply the OtE algorithm with $\rho_t = 0.5$ to 16 commercial batteries to investigate the times-to-charge and efficiencies of the batteries. The parameters of the batteries, i.e., the electrical parameters of the models in Figs. 1 and 2, and the parameters of the OCV function in (60), were calculated using experimental data and by applying the BFG algorithms in Refs. [3,4]. These parameters are listed in Tables 3 and 4 in the Appendix. Fig. 12 shows the TTC versus efficiency for different types of batteries. Among all batteries, Sam-EB575152 (Cell 3) has the lowest efficiency (90.73%). This can be attributed to the high resistance of this battery, which might be due to aging. Sam-EB504465 (Cell 4) has the highest TTC (102 min) and Nokia BP-4L (Cell 4) has the highest efficiency. Note

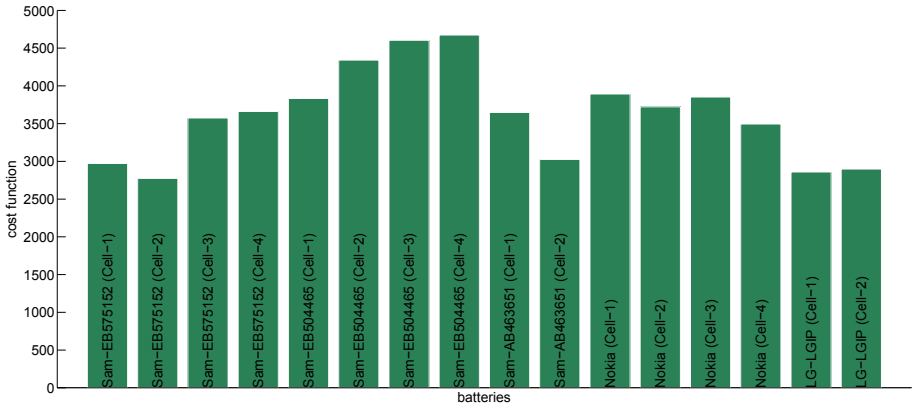

Fig. 13. Cost function for different battery types at 25 °C, $\rho_t = 0.5$.

Please cite this article in press as: A. Abdollahi, et al., Journal of Power Sources (2015), http://dx.doi.org/10.1016/j.jpowsour.2015.02.075

that the cells of the same battery are close to each other in terms of efficiency and TTC. Considering all the cells of a battery, we can say that LG-LGIP cells (circle markers) have the highest efficiency (91.4%). Fig. 13 shows the cost function values of $J_{tE} = \rho_t J_t + J_E$. When TTC is weighted with weight value of $\rho_t = 0.5$, Sam-EB575152 (Cell 2) has the best performance.

5. Conclusion

The optimal charging problem involving a weighted combination of time-to-charge (TTC), energy loss (EL) and temperature rise index (TRI) was considered. The optimal TTC and EL solution (OtE) is found to be the well-known CC–CV strategy with the value of current in the CC stage being a function of the ratio of weighting on TTC and EL and also the resistance of battery. To the best of our knowledge, this is the first time that it is proved that the well-known CC–CV charging profile is the optimal solution of a particular optimization problem, namely, the problem of minimizing the weighted sum of time-to-charge and energy loss. In addition, an analytical solution for the optimal TTC, EL and TRI, referred to as OtET, was developed. Due to similarity of the structure of the OtE and OtET solutions, a near-optimal version of OtET was developed (referred to as NOtET). The NOtET is a CC–CV strategy with the value of current in the CC stage being a function of the ratio of weighting on TTC and EL, the resistance of the battery and the effective thermal resistance. A number of simulations were conducted to evaluate the effect of weighting parameters. Finally, extensive results on industrial batteries from LG, Nokia and Samsung were presented.

Acknowledgments

The work reported in this paper was partially supported by NSF grants ECCS-0931956 (NSF CPS), ECCS-1001445 (NSF GOALI), CCF-1331850 (NSF CyberSEES), ARO grant W911NF-10-1-0369, and ONR grant N00014-10-1-0029. We thank NSF, ARO and ONR for their support of this work. Y. Bar-Shalom was partially supported by Grant ARO W991NF-10-1-0369. Any opinions expressed in this paper are solely those of the authors and do not represent those of the sponsors.

Nomenclature

a, b	coefficients in temperature model, (42,43)
C_{batt}	capacity, (2)
c_h	parameter in coulomb counting, (1)
$C_{h,batt}$	heat capacity of the battery in $J/(kg\cdot K)$, (42)
CC	constant current
CV	constant voltage
Δ	sampling time, (2)
EL	energy loss
η	charging efficiency
$G_{eq}[k]$	conductance equal to reciprocal of $R_{eq}[k]$, (56)
$H[k]$	Hamiltonian function, (16)
$i[k]$	charging current, (1)
$i^*[k]$	optimal current, (28)
$i^*[k\|k_1]$	optimal current given k_1
J_E	energy loss cost function, (3)
J_T	temperature rise cost function, (46)
J_t	time to charge cost function, (3)
J_{tE}	objective function as a combination of TTC and EL cost functions, (12)
J_{tE*}	partially optimized cost function, (30)
J_{tET}	cost function including time-to-charge (TTC), energy loss (EL), and temperature rise index (TRI), (46)
$J_E^*(k_1)$	minimum energy loss cost function as a function of k_1 (given k_1), (29)
$J_{tE}^*(k_1^*)$	optimized cost function
k	time index, (1)
k_1^*	optimal final time for constant-current charging stage, (34)
$k_1^{\mp}$	solutions to partially optimized cost function, (33)
k_1	time when terminal voltage reaches maximum allowed value, (11)
k_f	final value of time index, (3)
L	Lagrangian function, (55)
$\lambda[k]$	co-state variable, (18)
m_{batt}	battery mass in kg, (42)
NOtET	near optimal TTC, energy loss, and temperature
$OCV(z)$	open circuit voltage, (60)
OtE	optimal time-to-charge and energy loss
OtET	optimal TTC, energy loss, and temperature rise
R_0	resistance in model I of battery as shown in Fig. 1, (3)
R_{Eff}	effective thermal resistance in K/W, (53)
$R_{eq}[k]$	heating equivalent resistance added to the battery resistance, (52)
$R_T[k]$	heating equivalent resistance, (52)
ρ_t	ratio of weight of TTC cost function to weight of EL cost function, (12)
s	state of charge, (1)
s_0	initial SOC, (4)
s_1	state of charge when terminal voltage reaches maximum allowed value, (11)
s_{kf}	final SOC, (4)
T	battery core temperature in kelvin, (41)
T_{amb}	ambient temperature in kelvin, (41)
$\tilde{T}[k]$	temperature rise, (44)
TTC	time-to-charge
$v[k]$	terminal voltage of battery, (38)
V_0	open-circuit voltage, (5)
v_c	voltage corresponding to SOC of 1, (8)
w_E	weight for energy loss cost function, (3)
w_t	weight for time to charge cost function, (3)
$z(s)$	parameter relating OCV to SOC, (59)

Appendix

The following tables show the parameters of the equivalent electrical circuit model III for different commercial batteries.

Table 3
Electrical parameters of model III for commercial batteries.

Make	Model	Cell#	R_0 (mΩ)	R_1 (mΩ)	C_1 (F)	α	C_{batt} (Ah)
Samsung	EB575152	1	253	106	4581	0.997934	1.1875
Samsung	EB575152	2	209	94	5203	0.997962	1.2187
Samsung	EB575152	3	418	58	6222	0.99724	1.2001
Samsung	EB575152	4	200	142	3046	0.997689	1.485
Samsung	EB504465	1	259	106	4598	0.997941	1.5001
Samsung	EB504465	2	268	168	2493	0.997615	1.5293
Samsung	EB504465	3	272	211	1680	0.997186	1.5261
Samsung	EB504465	4	287	224	1589	0.997189	1.4831
Samsung	AB463651	1	451	198	2100	0.997597	0.9791
Samsung	AB463651	2	294	214	1950	0.997602	0.9614
Nokia	BP-4L	1	263	100	5031	0.998012	1.5514
Nokia	BP-4L	2	264	64	8141	0.99808	1.5691
Nokia	BP-4L	3	258	95	5306	0.998028	1.5612
Nokia	BP-4L	4	228	50	10502	0.998106	1.613
LG	LGIP	1	264	101	4747	0.997919	1.1141
LG	LGIP	2	297	76	6654	0.998021	1.1121

Table 4
OCV parameters for commercial batteries.

Make	Model	Cell#	OCV parameters							
			K_0	K_1	K_2	K_3	K_4	K_5	K_6	K_7
Samsung	EB575152	1	−1.1288	65.0931	−10.5332	1.0640	−0.0457	−52.2654	94.1916	−0.7417
Samsung	EB575152	2	−1.6976	68.3306	−11.1189	1.1290	−0.0487	−54.5366	98.4237	−0.7882
Samsung	EB575152	3	−1.0802	68.3600	−11.0617	1.1178	−0.0480	−55.3010	99.0817	−0.8059
Samsung	EB575152	4	−4.3113	22.9007	−4.2921	0.4926	−0.0239	−10.3460	27.2251	0.0226
Samsung	EB504465	1	0.0218	54.9000	−9.1299	0.9668	−0.0442	−44.6447	78.9622	−0.7934
Samsung	EB504465	2	1.8254	61.0951	−10.0031	1.0470	−0.0474	−52.6013	89.7801	−1.0640
Samsung	EB504465	3	0.2510	55.0370	−9.1256	0.9634	−0.0439	−45.0942	79.3945	−0.8297
Samsung	EB504465	4	2.9648	59.8808	−9.7283	1.0127	−0.0457	−52.9562	88.9546	−1.1311
Samsung	AB463651	1	−1.6972	41.8528	−7.0700	0.7522	−0.0343	−30.6508	58.1983	−0.4098
Samsung	AB463651	2	−1.2526	40.3216	−6.7711	0.7166	−0.0326	−29.7536	56.3932	−0.3814
Nokia	BP-4L	1	−3.2203	51.9246	−8.8187	0.9344	−0.0421	−38.1050	71.7162	−0.5991
Nokia	BP-4L	2	−2.7537	52.9707	−8.9327	0.9407	−0.0422	−39.6357	73.7620	−0.6418
Nokia	BP-4L	3	−3.2084	51.8554	−8.7993	0.9314	−0.0419	−38.0572	71.6483	−0.5996
Nokia	BP-4L	4	−2.7140	60.3626	−10.0810	1.0533	−0.0469	−46.2542	85.0092	−0.7139
LG	LGIP	1	0.5267	61.5448	−10.1553	1.0682	−0.0485	−51.2165	89.3849	−0.9091
LG	LGIP	2	0.4788	59.0975	−9.7677	1.0290	−0.0468	−48.9737	85.6643	−0.8748

References

[1] E. l. Alami, N.A. Ouansafi, N. Znaidi, On the discrete linear quadratic minimum-time problem, J. Frankl. Inst. 335 (3) (1998) 525–532.
[2] R.A. Aliev, R.R. Aliev, B. Guirimov, K. Uyar, Dynamic data mining technique for rules extraction in a process of battery charging, Appl. Soft Comput. 8 (3) (June 2008).
[3] B. Balasingam, B. Pattipati, G. Avvari, K. Pattipati, Y. Bar-Shalom, A robust approach to battery fuel gauging, part I: real time model identification, J. Power Sources 272 (Dec. 2014) 1142–1153.
[4] B. Balasingam, B. Pattipati, G. Avvari, K. Pattipati, Y. Bar-Shalom, A robust approach to battery fuel gauging, part II: real time capacity estimation, J. Power Sources 269 (Dec. 2014) 949–961.
[5] D.P. Bertsekas, Nonlinear Programming, Athena Scientic, Belmont, MA, 1999.
[6] L.R. Chen, A design of an optimal battery pulse charge system by frequency-varied technique, IEEE Trans. Ind. Electron. 54 (1) (Feb. 2007), p. 398,405.
[7] L.R. Chen, Design of duty-varied voltage pulse charger for improving Li-ion battery-charging response, IEEE Trans. Ind. Electron. 56 (2) (Feb. 2009).
[8] L.R. Chen, R.C. Hsu, Chuan-Sheng Liu, A design of a grey-predicted Li-ion battery charge system, IEEE Trans. Ind. Electron. 55 (10) (Oct. 2008), p. 3692, 3701.
[9] R.C. Cope, Y. Podrazhansky, The art of battery charging, in: Battery Conference on Applications and Advances, 1999. The Fourteenth Annual, IEEE, 1999, pp. 233–235.
[10] G. Guo, P. Xu, Z. Bai, S. Zhou, G. Xu, B. Cao, Optimization of Ni-MH battery fast charging in electric vehicles using dynamic data mining and ANFIS, in: Advanced Intelligent Computing Theories and Applications. With Aspects of Artificial Intelligence, Springer, Berlin Heidelberg, 2008, pp. 468–475.
[11] X. Hu, S. Li, H. Peng, F. Sun, Charging time and loss optimization for LiNMC and $LiFePO_4$ batteries based on equivalent circuit models, J. Power Sources 239 (2013) 449–457.
[12] Y.H. Liu, Y.F. Luo, Search for an optimal rapid-charging pattern for Li-ion batteries using the Taguchi approach, IEEE Trans. Ind. Electron. 57 (12) (Dec. 2010).
[13] P.H.L. Notten, J.H.G.O. het Veld, J.R.G. Van Beek, Boost charging Li-ion batteries: a challenging new charging concept, J. Power Sources (July 2005) 89–94.
[14] A.A. Pesaran, A. Vlahinos, S.D. Burch, Thermal performance of EV and HEV battery modules and packs, in: Proceedings of the 14th International Electric Vehicle Symposium, Orlando, Florida, December 15–17, 1997.
[15] A.A. Pesaran, Battery thermal models for hybrid vehicle simulations, J. Power Sources 110 (2) (2002) 377–382.
[16] P. Petchjatuporn, N. Khaehintung, K. Sunat, P. Sirisuk, W. Kiranon, Implementation of GA-trained GRNN for intelligent fast charger for Ni-Cd batteries, Power Electron. Motion Control Conf. (2006) 1–5.
[17] B.K. Purushothaman, U. Landau, Rapid charging of lithium-ion batteries using pulsed currents: a theoretical analysis, J. Electrochem. Soc. 153 (3) (2006).
[18] E.I. Verriest, F.L. Lewis, On the linear quadratic minimum-time problem, IEEE Trans. Auto. Control 36 (7) (1991) 859–863.
[19] J. Yan, G. Xu, H. Qian, Y. Xu, Z. Song, Model predictive control-based fast charging for vehicular batteries, Energies 4 (8) (2011) 1178–1196.
[20] J. Zhang, J. Yu, C. Cha, H. Yang, The effects of pulse charging on inner pressure and cycling characteristics of sealed Ni/MH batteries, J. Power Sources (September 2004) 180–185.
[21] T. Ikeya, N. Sawada, S. Takagi, J. Murakami, K. Kobayashi, et al., Multi-step constant-current charging method for electric vehicle, valve-regulated, lead/acid batteries during night time for load-leveling, J. Power Sources 75 (1) (Sep. 1998) 101–107.
[22] T. Ikeya, N. Sawada, J. Murakami, K. Kobayashi, et al., Multi-step constant-current charging method for an electric vehicle nickel/metal hydride battery with high-energy efficiency and long cycle life, J. Power Sources 105 (1) (Mar. 2002) 6–12.
[23] T.T. Vo, X. Chen, W. Shen, A. Kapoor, New charging strategy for lithium-ion batteries based on the integration of Taguchi method and state of charge estimation, J. Power Sources 273 (2015) 413–422.
[24] Y.H. Liu, J.H. Teng, Y.C. Lin, Search for an optimal rapid charging pattern for lithium-ion batteries using ant colony system algorithm, Ind. Electron. IEEE Trans. 52 (5) (2005) 1328–1336.
[25] Z. Guo, B.Y. Liaw, X. Qiu, L. Gao, C. Zhang, Optimal charging method for lithium ion batteries using a universal voltage protocol accommodating aging, J. Power Sources 274 (2015) 957–964.
[26] Z. Guo, X. Qiu, G. Hou, B.Y. Liaw, C. Zhang, State of health estimation for lithium ion batteries based on charging curves, J. Power Sources 249 (2014) 457–462.
[27] J. Li, E. Murphy, J. Winnick, P.A. Kohl, The effects of pulse charging on cycling characteristics of commercial lithium-ion batteries, J. Power Sources 102 (1) (2001) 302–309.

Please cite this article in press as: A. Abdollahi, et al., Journal of Power Sources (2015), http://dx.doi.org/10.1016/j.jpowsour.2015.02.075